Backbone Cyclic Peptide Inhibitors of Protein Kinase B (PKB/Akt)

Yftah Tal-Gan,[†] Mattan Hurevich,[†] Shoshana Klein,[‡] Avraham Ben-Shimon,[||] David Rosenthal,[†] Carina Hazan,[†] Deborah E. Shalev,[§] Masha Y. Niv,[||] Alexander Levitzki,[‡] and Chaim Gilon*,[†]

[†]Institute of Chemistry, [‡]Unit of Cellular Signaling, Department of Biological Chemistry, The Alexander Silberman Institute of Life Sciences, and [§]The Wolfson Centre for Applied Structural Biology, The Hebrew University of Jerusalem, 91904 Jerusalem, Israel

[||]Institute of Biochemistry, Food Science and Nutrition, The Hebrew University, 76100, Rehovot, Israel

Ⓢ Supporting Information

ABSTRACT: Elevated levels of activated protein kinase B (PKB/Akt) have been detected in many types of cancer. Substrate-based peptide inhibitors have the advantage of selectivity due to their extensive interactions with the kinase-specific substrate binding site but often lack necessary pharmacological properties. Chemical modifications of potent peptide inhibitors, such as cyclization, may overcome these drawbacks while maintaining potency. We present an extensive structure—activity relationship (SAR) study of a potent peptide-based PKB/Akt inhibitor. Two backbone cyclic (BC) peptide libraries with varying modes of cyclization, bridge chemistry, and ring size were synthesized and evaluated for in vitro PKB/Akt inhibition. Backbone-to-backbone urea BC peptides were more potent than N-terminus-to-backbone amide BC peptides. Several analogues were up to 10-fold more active than the parent linear peptide. Some activity trends could be rationalized using computational surface mapping of the PKB/Akt kinase catalytic domain. The novel molecules have enhanced pharmacological properties which make them promising lead candidates.
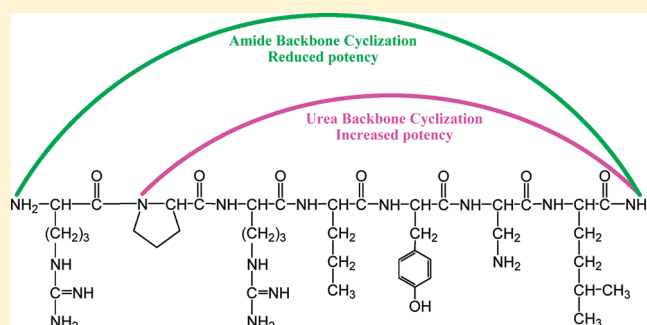
INTRODUCTION

Continuously activated protein kinase B (PKB/Akt) is associated with many types of human cancer, such as breast, colon, ovary, pancreas, head and neck, and prostate cancer.[1] PKB/Akt is therefore an attractive target for cancer therapy. Screening small molecules for enzyme inhibition is an accepted approach to discovering new drug lead compounds. Small molecular weight ATP-mimetic kinase inhibitors usually exhibit low selectivity toward the desired kinase.[2−8] A number of potent ATP-competitive inhibitors of PKB/Akt have been reported (reviewed in refs 9−11). All of these show off-target effects, especially inhibition of the closely related kinases PKA and PKC. Peptide inhibitors derived from the protein substrate have the potential to be kinase-selective because of multiple and specific interactions with the protein kinase binding site.[12−16] A series of peptides derived from a PKB/Akt substrate, the protein glycogen synthase kinase 3 (GSK3), were recently developed and their interactions with PKB/Akt were studied. The peptide Arg-Pro-Arg-Nva-Tyr-Dap-Hol **1** (PTR6154),[17] derived from the GSK3 substrate peptide segment Arg-Pro-Arg-Thr-Ser-Ser-Phe, showed potential as a selective PKB/Akt inhibitor.[17]

Linear peptides have drawbacks as drug candidates, such as poor bioavailability and rapid metabolism by proteolysis. Because of their structural flexibility, they can show nonselective receptor binding. Peptidomimetic analogues are designed to retain or enhance the desired biological effects of natural peptides while overcoming their undesirable properties. Many types of local and global modifications have been developed in order to form peptidomimetic compounds with improved pharmacological properties.[18−21] Cyclization is one of the most common strategies used to prepare peptide-based drugs. There are many ways to produce biopharmaceutical cyclic peptides, including metal cyclization,[22,23] metathesis-mediated cyclization,[24−26] amide cyclization,[27] and disulfide bridge cyclization.[28−33] Cyclization of natural bioactive peptides is not always feasible, however, because of the lack of suitable side chain functionalities for bridge formation or because the functional groups are essential for bioactivity.[34,35] The backbone cyclization methodology[36] overcomes these limitations by conferring long-range conformational constraints upon the peptide backbone, with minimal alterations to the native peptide side chains. Ring closure is achieved by functionalized alkyl spacers anchored to the peptide backbone. These spacers can be connected to another appropriate functionalized spacer, to a functional amino acid side chain on the peptide, or to the N- or C-terminus. Cyclization can thus be accomplished with minimal changes to the sequence that is required for bioactivity. Restricting the conformational space of peptide structures by cyclization often results in inactive peptides; thus, libraries must be screened to select cyclic peptide(s) with the desired biological activity.[37−40] Conformational libraries of backbone cyclic peptides can be prepared by varying four

Table 1. Chemical Shift Assignment and Local Root-Mean-Square Deviation

	(A) [1]H Chemical Shift Assignment of **1** over 15-Member Low-Energy Ensemble			
	$^3J_{HN\text{-}H\alpha}$ (Hz)	HN (ppm)	Hα (ppm)	Hβ (ppm_	others (ppm)
Arg1			4.22	1.80	Hγ 1.58; Hδ 3.07
Pro2		8.89	4.37	2.24, 1.75	Hγ 1.92; Hδ 3.66, 3.47
Arg3	5.3	8.63	4.11	1.63	Hγ 1.53, 1.46; Hδ 3.06
Nva4	5.7	8.36	4.17	1.52	Hγ 1.17, 1.11; Hδ 0.76
Tyr5	4.6	8.34	4.35	2.87, 2.80	Hδ 6.98; Hε 6.69
Dap6	3.7	8.39	4.41	2.87	
Hol7	5.3	8.30	4.02	1.68, 1.59	Hγ 1.12; Hδ 1.43; Hε 0.75

(B) Local Three-Residue Backbone rmsd					
			residue		
	1−3	2−4	3−5	4−6	5−7
rmsd	0.5	0.6	0.4	0.0	0.5
length (Å)	9	6	3	5	2

parameters: the mode of cyclization (i.e., backbone to backbone, backbone to amino terminus, backbone to carboxy terminus, or backbone to side chain), bridge position (determining which of the backbone atoms will be a part of the ring), ring size (derived from the size of the functionalized spacers), and bridge chemistry (defined by the type of chemical functions that exist on the bridge, namely, the chemistry of the bond used for cyclization and the position of these chemical entities on the bridge). Active backbone cyclic peptides discovered by library screening have been shown to have enhanced selectivity,[41] potency,[42] bioavailability, and metabolic stability compared to linear peptides.[43,44]

The importance of the side chain orientations and backbone interactions for inhibitory activity has been highlighted in previous studies of peptidomimetic analogues of **1**, which included mono-N^α-methylation and peptoid and azapeptide scans.[45,46] This prompted us to prepare backbone cyclic analogues, based on the parent peptide **1**, in an attempt to improve the druglike properties of **1** without losing its interactions with the target kinase. Recently, we introduced a new method for synthesizing backbone cyclic peptides, using a urea bridge for ring closure. In this procedure, we introduced two glycine derivatives of the type Fmoc-N^α-[(Alloc)-ω-aminoalkyl]glycine (termed Alloc glycine building unit, AGBU) and connected them via a urea bridge.[47] We have already described the preparation of four backbone cyclic peptides derived from **1** using urea backbone cyclization.[47]

The synthesis and structure—activity relationship (SAR) study was done on two backbone cyclic peptide libraries and their precyclic precursors, all based on the sequence of **1**. The activity of the peptides of the urea BC library was superior to that of the peptides of the amide BC library and included several analogues that were 10-fold more potent than the parent peptide, **1**. NMR and computational analyses were done to study the structural and biochemical basis of the observed potency trends. These provided insights into the activities of the library peptides and directions for future modifications.

■ RESULTS AND DISCUSSION

Structural NMR Study. In our procedure for building a urea backbone cyclic peptide, two AGBUs were introduced and connected via a urea bridge.[47] In order to choose the optimal
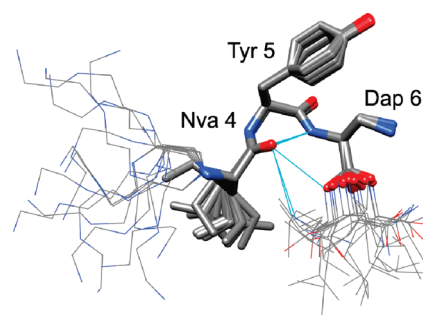

Figure 1. NMR-derived ensemble of 15 low energy representative structures of **1** superimposed over low local rmsd region of residues 4−6, showing H-bonds between all Nva4 O and Dap6 HN and additional ones between Nva 4 O and Hol 7 donor. Residues 1−3 are in backbone representation, and Hol7 is in wire representation.

residue to be replaced with an *N*-alkyl(amino functionalized)glycine residue for cyclization, structural NMR studies were performed on the parent peptide **1** (assignment in Table 1A, spectra in Supporting Information Figure 1). **1** gave a set of well-resolved spectra showing 22 intraresidual, 10 sequential, and 2 *i*,*i*+2 NOE interactions. The 50-conformation ensemble had no violations and a rmsd of 1.57 Å for the backbone atoms (bb) and 3.76 Å for the heavy atoms. Local rmsd values were calculated along the length of the peptide (Table 1B), and the 15-conformation low energy ensemble (Figure 1) was superimposed over the well-defined region of Nva4 to Dap6, which had a hydrogen bond between Nva4 O and Dap6 HN in all calculated conformations. Further hydrogen bonds between Nva4 O and Hol7 donor were also identified. The $^3J_{HNH\alpha}$ couplings in this molecule were all below 6 Hz, indicating the secondary turn conformation.

The low energy NMR-derived conformation of **1** was superimposed over the GSK3 substrate peptide within PKB/Akt (PDB code 1O6K) (Figure 2). The Arg3 residues of the substrate and the inhibitor overlap well, but Tyr5 of **1** clashes with ANP within PKB/Akt, suggesting that **1** might not only prevent GSK3 from binding to PKB/Akt but might also prevent ATP from entering its binding site. Additional clashes are seen between Arg1 and PKB/Akt. The N-terminus of **1** was found by NMR to be flexible

in solution and is likely to adopt a different conformation upon binding to the kinase, considering the strong binding site on PKB/Akt for the guanidino group of Arg1 (ref 48 and see computational section below).

Proline Modifications Library. The NMR results showed considerable flexibility in the N-terminal region of the proline residue, suggesting that **1** might be amenable to modifications in this region. Since proline usually induces local constraint, this site
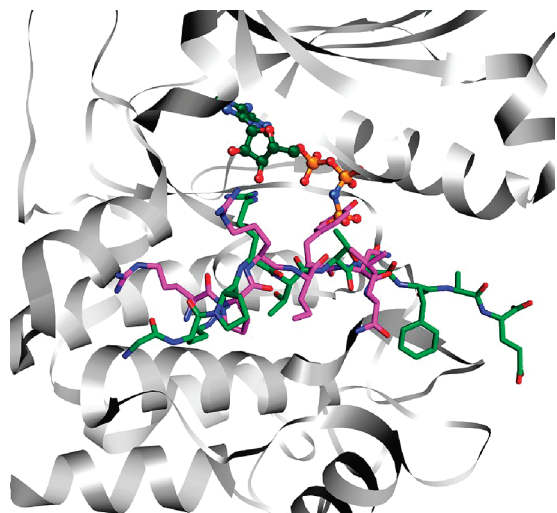

Figure 2. Low energy NMR-derived conformation of **1** (magenta) superimposed over GSK3 (green) within PKB/Akt (gray ribbon, PDB code 1O6K). Tyr5 of **1** overlaps with ANP (stick and ball presentation) within PKB/Akt, suggesting possible mode of inhibition. Additional clashes are seen between Arg1 and PKB/Akt in this model, but the N-terminus region is very flexible.

was marked as a potential target for cyclization, which introduces a global constraint on the entire peptide sequence. A library in which Pro2 was replaced with various natural and artificial amino acids was prepared to examine the feasibility of replacing proline. Modifications included hydrophobic moieties, aromatic moieties, positive and negative charges, and D-amino acids. It is clear that proline (Table 2) can be replaced by either a positive or an aliphatic moiety without loss of potency. For example, **3** with an aliphatic residue (IC$_{50}$ = 0.95 μM) and **14** with a positively charged residue (IC$_{50}$ = 0.86 μM) have IC$_{50}$ values comparable to that of **1** (IC$_{50}$ = 0.94 μM). D-Amino acids and aromatic or negatively charged amino acid residues were less favored and usually resulted in decreased potency: for example, compare **8** with an aromatic residue (60% inhibition at 5 μM) and **12** with a negatively charged residue (68% inhibition at 5 μM) to **1** (87% inhibition at 5 μM). None of the library members showed increased potency relative to **1**. Taken together, these results indicate that Pro2 plays a role in stabilizing the PKB/Akt-bound peptide in the necessary conformation, but it can be replaced by other L-amino acids.

These results encouraged us to insert an *N*-alkyl(amino functionalized)glycine residue (a linear, positively charged moiety) in place of the proline. This replacement did not cause a major change in potency (Table 2, **18** and **19**).

Precyclic Library YM*n-m*. The precyclic library, YM*n-m*, was prepared as the first step for urea backbone cyclization. The library was synthesized by introducing two AGBUs of varying chain lengths. In accordance with the mutagenesis study summarized in Table 2, the first AGBU replaced the proline residue (cyclic N-alkylated amino acid) of **1**. The second AGBU was added to the carboxy terminus of the peptide, since in our earlier studies we found that all of the C-terminal amino acids are essential for potency.[45,46] In the notation YM*n-m*, the chain

Table 2. Inhibitory Activity and IC$_{50}$ of the Proline Modifications Library[a]

compd	name	structure	% inhibition (5 μM)	IC$_{50}$ (μM) (95% confidence)
1		H-Arg-Pro-Arg-Nva-Tyr-Dap-Hol-NH$_2$	87 ± 2	0.94 (0.78−1.14)
2	YTG10[b]	H-Arg-**DPro**-Arg-Nva-Tyr-Dap-Hol-NH$_2$	NI	ND
3	YTG11[b]	H-Arg-**Cha**-Arg-Nva-Tyr-Dap-Hol-NH$_2$	85 ± 2	0.95 (0.81−1.13)
4	YTG12[b]	H-Arg-**Nle**-Arg-Nva-Tyr-Dap-Hol-NH$_2$	82 ± 1	ND
5	YTG13[b]	H-Arg-**Nva**-Arg-Nva-Tyr-Dap-Hol-NH$_2$	80 ± 1	ND
6	YTG14[b]	H-Arg-**Ala**-Arg-Nva-Tyr-Dap-Hol-NH$_2$	81 ± 2	ND
7	YTG15[b]	H-Arg-**DAla**-Arg-Nva-Tyr-Dap-Hol-NH$_2$	NI	ND
8	YTG16[b]	H-Arg-**Phe**-Arg-Nva-Tyr-Dap-Hol-NH$_2$	60 ± 3	ND
9	YTG17[b]	H-Arg-**DPhe**-Arg-Nva-Tyr-Dap-Hol-NH$_2$	NI	ND
10	YTG18[b]	H-Arg-**Tyr**-Arg-Nva-Tyr-Dap-Hol-NH$_2$	74 ± 2	ND
11	YTG19[b]	H-Arg-**DTyr**-Arg-Nva-Tyr-Dap-Hol-NH$_2$	NI	ND
12	YTG20[b]	H-Arg-**Asp**-Arg-Nva-Tyr-Dap-Hol-NH$_2$	68 ± 1	ND
13	YTG21[b]	H-Arg-**DAsp**-Arg-Nva-Tyr-Dap-Hol-NH$_2$	NI	ND
14	YTG22[b]	H-Arg-**Dap**-Arg-Nva-Tyr-Dap-Hol-NH$_2$	94 ± 1	0.86 (0.62−1.23)
15	YTG23[b]	H-Arg-**DDap**-Arg-Nva-Tyr-Dap-Hol-NH$_2$	32 ± 1	ND
16	YTG24[b]	H-Arg-**Lys**-Arg-Nva-Tyr-Dap-Hol-NH$_2$	92 ± 4	2.15 (1.77−2.61)
17	YTG25[b]	H-Arg-**DLys**-Arg-Nva-Tyr-Dap-Hol-NH$_2$	27 ± 2	ND
18	YTG26[b]	H-Arg-**GBU2**-Arg-Nva-Tyr-Dap-Hol-NH$_2$	84 ± 2	0.85 (0.51−1.53)
19	YTG27[b]	H-Arg-**GBU4**-Arg-Nva-Tyr-Dap-Hol-NH$_2$	84 ± 2	1.00 (0.40−2.49)

[a] PKB/Akt inhibition was determined according to radioactive kinase assay as previously described.[3] Inhibition at 5 μM inhibitor is shown as the percent reduction in PKB/Akt activity (0% inhibition = activity in the absence of inhibitor). IC$_{50}$ values and 95% confidence range (parentheses) were determined using Graphpad Prism 5 only for inhibitors that showed over 85% inhibition at 5 μM. NI = no inhibition. ND = not determined. GBU = *N*-alkyl(amino functionalized)glycine. [b] Compound code numbers from ref 49.

Table 3. Inhibitory Activity and IC$_{50}$ of the YMn-m Library^a
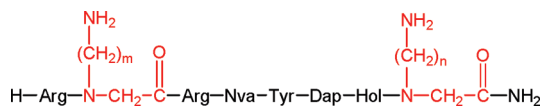
compd	name	m	n	% inhibition (0.625 μM)	IC$_{50}$ (μM) (95% confidence)
1	b			36 ± 2	0.94 (0.78−1.14)
20	YM2-2^c	2	2	57 ± 3	ND
21	YM2-3^c	3	2	76 ± 2	0.32 (0.25−0.42)
22	YM2-4^c	4	2	84 ± 1	0.22 (0.10−0.48)
23	YM2-6^c	6	2	83 ± 4	0.32 (0.22−0.47)
24	YM3-2^c	2	3	76 ± 4	0.25 (0.12−0.52)
25	YM3-3^c	3	3	90 ± 4	0.13 (0.06−0.28)
26	YM3-4^c	4	3	91 ± 2	0.15 (0.09−0.28)
27	YM3-6^c	6	3	87 ± 4	0.11 (0.02−0.69)
28	YM4-2^c	2	4	84 ± 4	0.176 (0.16−0.19)
29	YM4-3^c	3	4	96 ± 2	0.128 (0.127−0.129)
30	YM4-4^c	4	4	91 ± 3	0.13 (0.06−0.28)
31	YM4-6^c	6	4	88 ± 3	0.16 (0.08−0.32)
32	YM6-2^c	2	6	42 ± 1	ND
33	YM6-3^c	3	6	51 ± 3	ND
34	YM6-4^c	4	6	60 ± 1	ND
35	YM6-6^c	6	6	57 ± 1	ND

^{a} PKB/Akt inhibition was determined according to radioactive kinase assay as previously described.[3] Inhibition at 0.625 μM inhibitor is shown as the percent reduction in PKB/Akt activity (0% inhibition = activity in the absence of inhibitor). IC$_{50}$ values and 95% confidence range (parentheses) were determined using Graphpad Prism 5 only for inhibitors that showed over 75% inhibition at 0.625 μM. ND = not determined. ^{b} H-Arg-Pro-Arg-Nva-Tyr-Dap-Hol-NH$_2$. ^{c} Compound code numbers from ref 49.

length of the ABGU replacing the proline is represented by m, and the chain length of the C-terminal AGBU is represented by n.

In general, the precyclic library (Table 3) exhibited better PKB/Akt inhibition than **1**, with some peptides having 10-fold lower IC$_{50}$ values: e.g., **27** (IC$_{50}$ = 0.11 μM) and **30** (IC$_{50}$ = 0.13 μM). The additional positive charge at the C-terminus improved potency. Moreover, the chain length n of the C-terminal AGBU had a greater effect on potency than the chain length m of the AGBU at position 2. The most potent compounds had n = 3 or n = 4, while there was a slight decrease in potency for n = 2. All peptides with n = 6 had significantly decreased potencies.

Cyclic Urea BC Library c(YMn-m). The urea BC library, c(YMn-m), was synthesized by cyclization of the precursors, Fmoc-YMn-m, from the penultimate step of synthesis of the precyclic library. Table 4 shows the in vitro inhibitory activity of the c(YMn-m) library. These data were evaluated by addressing each of the following parameters: the AGBU at the carboxy terminus (peptides having the same n); the AGBU at position 2 (peptides having the same m); the overall ring size of the peptides. The value of n exhibited a direct influence on the potency, but no definite conclusions could be drawn regarding overall ring size. All members of the sublibrary with n = 2 had poor potencies, whereas the cyclic sublibraries with n = 3, n = 4, and n = 6 were more potent than **1**, with the exceptions of **42** and **51**. No similar generalization could be made with regard to the values of m. Evaluation according to ring size also showed no conclusive pattern, and potencies varied significantly between

peptides of the same ring size (e.g., **37** versus **40** where ring size is 27, **42** versus **45** where ring size is 29, **39** versus **46** and **48** where ring size is 30). The four BC peptides with ring sizes of 31 or 32 atoms were all potent. Overall, neither a preferred ring size nor a preferred urea bond position (represented by different combinations of n and m with the same total ring size) was identified. The critical parameter determining potency is the bioactive conformation actually obtained by the molecule, which is dependent on both ring size and urea bond position. Thus, in some cases, the combination of ring size and urea position apparently resulted in a peptide that adopted a bioactive conformation, retaining the parental potency (e.g., **40** (IC$_{50}$ = 0.92 μM)) or even improving upon it (e.g., **43** (IC$_{50}$ = 0.16 μM) and **46** (IC$_{50}$ = 0.17 μM)).

A comparison of the precyclic and cyclic libraries revealed that a few of the molecules in the precyclic library were more active than their cyclic counterparts. This may be due to the additional positive charges on the precyclic analogues, which are absent from the cyclic analogues. Alternatively, the decreased conformational freedom brought about by cyclization may destabilize the extended conformations of the peptides that are compatible with protein binding.

Deleted Arginine 1 Derivatives, YM2-mNR and c(YM2-mNR). Coupling Arg1 to the AGBU was incomplete in the precyclic and urea BC sublibraries YM2-m and c(YM2-m). By use of a combinatorial approach, the derivatives lacking Arg1, namely, des-Arg1 YM2-m and des-Arg1 c(YM2-m), were separated and evaluated for PKB/Akt inhibition. The linear des-Arg1 peptides, YM2-mNR (Table 5), were significantly less potent than the corresponding YM2-m peptides (Table 3) which included the Arg1 residue (e.g., **22** 84% inhibition at 0.625 μM and IC$_{50}$ = 0.22 μM versus **54** 66% inhibition at 5 μM). These results suggest that Arg1 plays a significant role in site recognition and are in accordance with peptide/kinase structural data (structures 1O6K, 1O6L),[50] the importance of Arg1 in PKB/Akt substrate peptides as manifested in the PKB/Akt consensus motif RXRXXS/T,[51,52] and the highly favorable calculated energy of binding of Arg1 to PKB/Akt [ref 48 and see below].

Surprisingly, unlike the linear peptides, the cyclic des-Arg1 peptides, c(YM2-mNR) (Table 6), showed enhanced potencies compared to the corresponding cyclic peptides which included the Arg1 residue c(YM2-m) (Table 4) (e.g., **37** 54% inhibition at 5 μM versus **57** 84% inhibition at 0.625 μM and IC$_{50}$ = 0.24 μM). The des-Arg1 c(YM2-mNR) peptides with the smallest ring sizes and the most constrained conformations were the most potent. It is unlikely that the urea moiety in the bridge can compensate for the loss of the guanidine entity, considering the constrained conformation and the great difference between the urea bridge and the arginine residue. Arg1 may form intramolecular interactions that are detrimental for binding to PKB/Akt, in the context of the small cyclic peptide. However, this hypothesis requires further study.

Amide BC Library c(DRn-m). An amide BC library was built in parallel to the urea BC library, c(DRn-m), where m represents the chain length of the dicarboxylic acid linker and n represents the chain length of the C-terminal AGBU. All the peptides of the amide BC library were found to be significantly less potent than **1** (Table 7). These results agree with our previous SAR studies which showed that a free N-terminal amine is favored for maintaining high levels of potency.[45] It is therefore not surprising that these peptides, in which the amino termini are blocked in the amide form, did not maintain the potency of the parent peptide, **1**.

In general, peptides in which the free N-terminal amine is important for activity are hindered by BN−AT amide bond cyclization that interferes with the N-terminal amine. The urea BC library, with a BN−BN mode of cyclization, showed better

Table 4. Inhibitory Activity and IC$_{50}$ of the c(YMn-m) Library^a
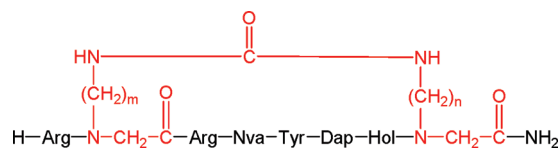
compd	name	m	n	bridge size	ring size	% inhibition (5 μM)	IC$_{50}$ (μM) (95% confidence)
1	b					87 ± 2	0.94 (0.78−1.14)
36	c(YM2-2)^c	2	2	7	26	30 ± 4	ND
37	c(YM2-3)^c	3	2	8	27	54 ± 4	ND
38	c(YM2-4)^c	4	2	9	28	84 ± 3	ND
39	c(YM2-6)^c	6	2	11	30	68 ± 4	ND
40	c(YM3-2)^c	2	3	8	27	98 ± 1d	0.92 (0.58−1.45)d
41	c(YM3-3)^c	3	3	9	28	98 ± 1d	0.59 (0.48−0.73)d
42	c(YM3-4)^c	4	3	10	29	54 ± 2d	NDd
43	c(YM3-6)^c	6	3	12	31	100 ± 1d	0.16 (0.03−0.77)d
44	c(YM4-2)^c	2	4	9	28	98 ± 1	0.282 (0.278−0.286)
45	c(YM4-3)^c	3	4	10	29	92 ± 1	ND
46	c(YM4-4)^c	4	4	11	30	100 ± 2	0.17 (0.10−0.29)
47	c(YM4-6)^c	6	4	13	32	100 ± 1	0.28 (0.23−0.35)
48	c(YM6-2)^c	2	6	11	30	100 ± 2	0.29 (0.21−0.39)
49	c(YM6-3)^c	3	6	12	31	100 ± 2	0.32 (0.27−0.37)
50	c(YM6-4)^c	4	6	13	32	94 ± 1	ND
51	c(YM6-6)^c	6	6	15	34	39 ± 1	ND

^{a} PKB/Akt inhibition was determined according to radioactive kinase assay as previously described.[3] Inhibition at 5 μM inhibitor is shown as the percent reduction in PKB/Akt activity (0% inhibition = activity in the absence of inhibitor). IC$_{50}$ values and 95% confidence range (parentheses) were determined using Graphpad Prism 5 only for inhibitors that showed over 95% inhibition at 5 μM. ND = not determined. ^{b} H-Arg-Pro-Arg-Nva-Tyr-Dap-Hol-NH$_2$. ^{c} Compound code numbers from ref 49. ^{d} Data from ref 47.

**Table 5. Inhibitory Activity of the YM2-mNR Derivatives^a**
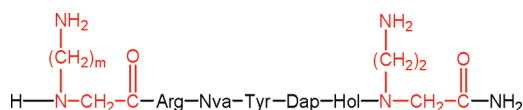
compd	name	m	n	% inhibition (5 μM)
1	b			87 ± 2
52	YM2-2NR^c	2	2	67 ± 1
53	YM2-3NR^c	3	2	63 ± 3
54	YM2-4NR^c	4	2	66 ± 4
55	YM2-6NR^c	6	2	64 ± 2

^{a} PKB/Akt inhibition was determined according to radioactive kinase assay as previously described.[3] Inhibition at 5 μM inhibitor is shown as the percent reduction in PKB/Akt activity (0% inhibition = activity in the absence of inhibitor). ^{b} H-Arg-Pro-Arg-Nva-Tyr-Dap-Hol-NH$_2$. ^{c} Compound code numbers from ref 49.

potencies than the amide BC library with a BN−AT mode of cyclization, demonstrating the effects of the mode of cyclization and of the bridge chemistry on the inhibitory activity. Furthermore, urea bond cyclization is more adaptable than amide bond cyclization, as it allows peptide elongation beyond the point of cyclization.[47] These results demonstrate that wide screening of BC peptide libraries, employing a hierarchical scan not only of ring size and chemistry but also of mode of cyclization, can play a dramatic role in the discovery of drug leads.

Computational Surface Mapping of the PKB/Akt Catalytic Domain. ANCHORSMAP[48,53] was used to discover potential binding positions for positively charged moieties on the surface of PKB/Akt. ANCHORSMAP is a novel computational mapping approach that was specifically designed for detecting "anchoring spots", which are binding positions of amino acid probes that stabilize protein−protein and protein−peptide complexes.[53] Figure 3 presents the five top ranking Arg-anchoring spots and five top ranking Lys-anchoring spots, as detected by ANCHORSMAP on the entire surface of the apo (unbound) structure of the kinase domain of PKB/Akt (3D0E.pdb). In addition to the known binding position for P-3 Arg (corresponding to Arg3 in **1**), which is characteristic of most basophilic kinases including PKB/Akt,[54] ANCHORSMAP detected three additional Arg-anchoring spots (ranks 1−3) within the major groove of the kinase domain, which may be relevant for binding a substrate or a substrate-like peptide.

The top ranking Arg-anchoring spot in PKB/Akt is in a surface pocket that indeed accommodates the Arg residue from position P-5 of the GSK3β-peptide[50] which corresponds to Arg1 of **1**. A similar Arg-binding pocket is present in the crystal structure of a substrate-like inhibitory peptide, PKI, bound to PKA[55] and in several other basophilic kinases.[48] The same position is also the top ranking one for accommodating Lys residues. Interestingly, the same pocket contains an auxiliary Arg binding position, ranked 2, implying that it can potentially accommodate two independent positively charged moieties simultaneously. These results explain why potency can be improved by substituting Pro2 (corresponding to P-4) by positively charged residues, such as N-alkyl(amino functionalized)glycine.

Table 6. Inhibitory Activity and IC$_{50}$ of the c(YM2-mNR) Derivatives[a]
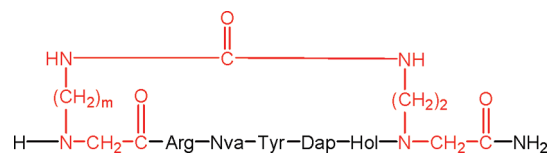
compd	name	m	n	bridge size	ring size	% inhibition (0.625 μM)	IC$_{50}$ (μM) (95% confidence)
1	b					36 $\pm$ 2	0.94 (0.78−1.14)
56	c(YM2-2NR)[c]	2	2	7	26	64 $\pm$ 4	0.39 (0.21−0.71)
57	c(YM2-3NR)[c]	3	2	8	27	84 $\pm$ 2	0.24 (0.10−0.58)
58	c(YM2-4NR)[c]	4	2	9	28	32 $\pm$ 4	ND
59	c(YM2-6NR)[c]	6	2	11	30	26 $\pm$ 2	ND

[a] PKB/Akt inhibition was determined according to radioactive kinase assay as previously described.[3] Inhibition at 0.625 μM inhibitor is shown as the percent reduction in PKB/Akt activity (0% inhibition = activity in the absence of inhibitor). IC$_{50}$ values and 95% confidence range (parentheses) were determined using Graphpad Prism 5 only for inhibitors that showed over 60% inhibition at 0.625 μM. ND = not determined. [b] H-Arg-Pro-Arg-Nva-Tyr-Dap-Hol-NH$_2$. [c] Compound code numbers from ref 49.

Table 7. Inhibitory Activity of the c(DRn-m) Library[a]
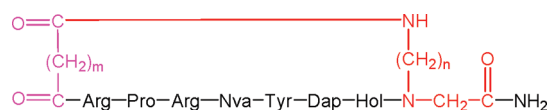
compd	name	m	n	bridge size	ring size	% inhibition (5 μM)
1	b					87 $\pm$ 2
60	c(DR4-2)[c]	2	4	9	31	13 $\pm$ 3
61	c(DR4-3)[c]	3	4	10	32	14 $\pm$ 2
62	c(DR4-4)[c]	4	4	11	33	18 $\pm$ 1
63	c(DR4-5)[c]	5	4	12	34	16 $\pm$ 2
64	c(DR6-2)[c]	2	6	11	33	25 $\pm$ 2
65	c(DR6-3)[c]	3	6	12	34	32 $\pm$ 3
66	c(DR6-4)[c]	4	6	13	35	30 $\pm$ 2
67	c(DR6-5)[c]	5	6	14	36	30 $\pm$ 4

[a] PKB/Akt inhibition was determined according to radioactive kinase assay as previously described.[3] Inhibition at 5 μM inhibitor is shown as the percent reduction in PKB/Akt activity (0% inhibition = activity in the absence of inhibitor). [b] H-Arg-Pro-Arg-Nva-Tyr-Dap-Hol-NH$_2$. [c] Compound code numbers from ref 49.

The third top ranking Arg binding spot and the second top ranking Lys binding spot are between two acidic residues in the N-lobe, Glu200 and Glu193 (numbers are according to the 3D0E structure), and can accommodate a positively charged residue at position P + 2 of the substrate or of a substrate-like peptide. A distance of 7 Å separates this binding spot from the Cβ atom at position P + 2 of GSK3β-peptide (PDB code 1O6K) (Figure 4). This explains why the optimal length for activity in the YMn-m library is n = 3 or n = 4; shorter or longer linkers would not bring the positively charged moiety of the AGBU into the binding spot without significant changes in backbone positioning. In **1**, there is no positively charged residue near the carboxy terminus that might fit into this binding spot. In the YMn-m library, the importance of the length n of the alkyl chain on the GBU at the C-terminus becomes greater than that of the length m of the alkyl chain on the GBU at position Pro2.

Helix αC in the N-lobe of PKB/Akt contains an additional acidic residue, Asp192, which together with Glu193 forms a
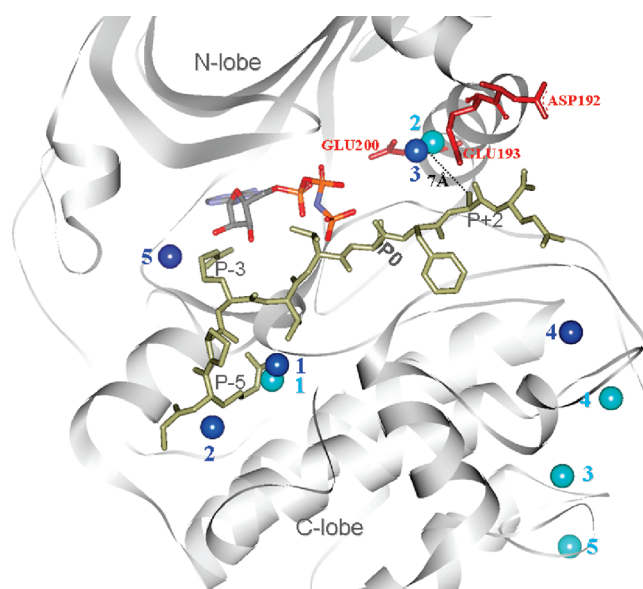

Figure 3. Arg-anchoring spots detected on the surface of PKB/Akt. The unbound structure of PKB/Akt (3D0E) and the superimposed GSK3β-peptide (1O6K) are shown in gray and olive green, respectively. ANP is shown in ball and stick representation. Acidic residues on helix αC are shown as red sticks. The top five predicted Arg and Lys anchoring spots are shown as blue and cyan spheres according to the positions of the Arg Cζ and Lys Nζ atoms, respectively. Blue and cyan numbers stand for ranking order.

solvent-exposed acidic environment. This acidic pair provides another binding site for a positive group and explains the preference for an amide rather than a carboxylic group at the C-terminus of the peptide, as reported previously.[45]

Overall, the computational analysis provides a reasonable explanation for the activity patterns observed in our SAR studies and demonstrates that this type of analysis can be of predictive value in planning future analogues.

■ CONCLUSIONS

Structure−activity relationships of a potent PKB/Akt substrate-based inhibitor, **1**,[17] were extensively studied. Using combinatorial
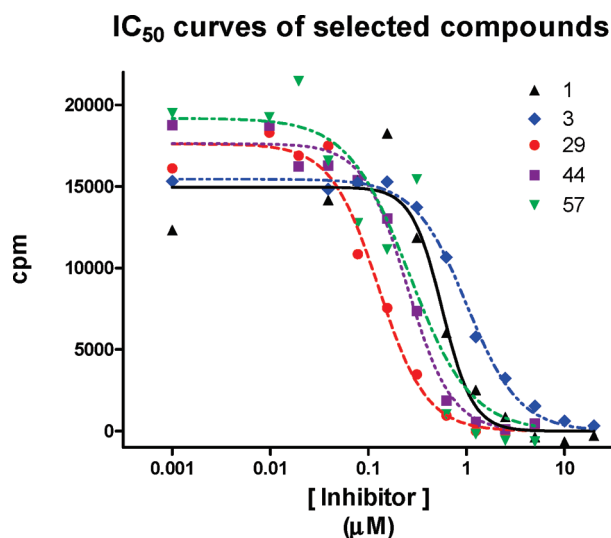
IC$_{50}$ curves of selected compounds

Figure 4. IC$_{50}$ curves of selected compounds produced using Graphpad Prism 5. Representative curves are shown.

BC libraries, we compared different modes of cyclization while screening the conformational space of the side chain residues. Our data highlight the importance of addressing all four BC conformational parameters: the mode of cyclization, ring position, ring size, and ring chemistry. The urea BC peptides were more potent than the amide BC peptides, and the chain length of the carboxyl AGBU was an important factor in potency.

NMR-derived structures of **1** gave an ensemble with a secondary turn conformation between Nva4 and Dap6. A low energy conformation was superimposed over GSK3 within PKB/Akt and showed only minor clashes in its flexible N-terminal region, confirming that **1** can indeed bind the PKB/Akt substrate binding site.

Our computational study was compatible with our experimental results and indicated that additional positive charges at the amino and carboxy termini may fit well into the substrate binding groove of PKB/Akt, a finding that explains the enhanced binding affinity to PKB/Akt of C-amidated peptides and of peptides carrying additional positive charges at the Pro2 and/or carboxy terminus position, including the precyclic analogues. To further explore the cyclic analogues, we plan to adapt the peptide docking algorithm[56] as well as the kinase/peptide molecular dynamics simulations[57] to cyclic peptides and to apply the computational analysis to study the conformational dynamics of the cyclic analogues within and outside the PKB/Akt environment.

Although most of the precyclic analogues showed enhanced PKB/Akt inhibition compared to **1**, the backbone cyclic peptides may be better drug leads, as they are expected to have improved metabolic stability and selectivity.[41,43,44] Six analogues, **25**, **27**, **29**, **30**, **43**, and **46**, out of a total of 66 library members, showed IC$_{50}$ < 0.2 μM. In addition to serving as drug leads, these analogues may also be useful probes for studying the precise mechanism of inhibition. The integrated chemical, structural, biochemical, and computational study presented here has provided novel inhibitors of PKB/Akt activity, as well as insights into kinase/peptide interactions and ideas for future cyclic peptide development.

■ EXPERIMENTAL SECTION

Chemistry: General. All starting materials were purchased from commercial sources and were used without further purification. Exact mass

spectra were recorded on an Agilent Technologies 6520B Accurate-Mass Q-TOF LC/MS instrument. MALDI-TOF spectra were recorded on a PerSeptive Biosystems MALDI-TOF MS instrument, using α-cyano-4-hydroxycinnamic acid as matrix. Preparative HPLC data were recorded at 220 nm on a RP-18 column (10 μm, 250 mm × 10 mm, 110 Å). Eluents A (0.05% TFA in TDW) and B (ACN) were used in a linear gradient (95% A → 75% A in 30 min) at a flow of 5 mL/min. Purity of all the compounds was determined by analytical HPLC and was recorded at 220 nm at a flow of 1 mL/min on a RP-18 column (5 μm, 250 mm × 4.6 mm, 110 Å). Eluents A (0.05% TFA in TDW) and B (ACN) were used in a linear gradient (95% A → 5% A in 35 min). The purity of all the compounds tested was ≥95%.

Peptide Design. All the peptides and peptidomimetics were synthesized using standard Fmoc SPPS procedures[58] on Rink amideMB-HA resin as the solid support. The urea BC library, designated c(YM*n*-*m*) (Table 4), was synthesized according to the procedures described by Hurevich et al.,[47] using combinations of various Alloc glycine building units (AGBUs), where *n* stands for the number of atoms in the N-alkyl chain on the glycine at the carboxy terminus (position 8) and *m* stands for the number of atoms in the N-alkyl chain of the glycine at position 2. Prior to cyclization, the resin was divided, and the precyclic analogues (namely, analogues that include the AGBU with ε-free amine and have no ring closure) were deprotected and purified as well (this library is designated YM*n*-*m*, Table 3). The coupling of Arg1 to the AGBU was incomplete in the c(YM2-*m*) and YM2-*m* sublibraries. By use of a combinatorial approach, the derivatives lacking Arg1, namely, des-Arg1 YM2-*m* and des-Arg1 c(YM2-*m*), were separated and evaluated for PKB/Akt inhibition. The des-Arg1 analogues are designated YM2-*m*NR and c(YM2-*m*NR) (Tables 5 and 6, respectively). The amide BC library, designated c(DR*n*-*m*) (Table 7), was synthesized as previously described[44,59] by using AGBU (*n* = 4 or 6) at the carboxy terminus and various dicarboxylic acid linkers (*m* = 2−5) that acetylate the amino terminus, for ring closure.

General Methods for SPPS. *Swelling.* The resin was swelled for at least 2 h in dichloromethane.

Fmoc Removal. The resin was treated with a solution of 20% piperidine in 1-methyl-2-pyrrolidinone (NMP) (2 × 20 min), then washed with NMP (5 × 2 min).

HBTU Coupling. Fmoc protected amino acids (1.5 equiv) were dissolved in NMP. N,N-Diisopropylethylamine (DIPEA) (1.5 equiv) and 1-hydroxybenzotriazole (HOBt) were added, and the mixture was cooled to 0 °C. 2-(1H-Benzotriazole-1-yl)-1,1,3,3-tetramethyluronium hexafluorophosphate (HBTU) (1.5 equiv) was added, and the mixture was preactivated by mixing for 10 min, added to the resin, and shaken for 1 h. The resin was washed with NMP (3 × 2 min).

Capping. The resin was treated with a solution of acetic anhydride (10 equiv) and DIPEA (7.15 equiv) in dimethylformamide (DMF) for 20 min and washed with NMP (3 × 2 min).

HATU Coupling. Fmoc protected amino acids (1.5 equiv) were dissolved in NMP. DIPEA (1.5 equiv) and 1-hydroxy-7-azabenzotriazole (HOAt) were added, and the mixture was cooled to 0 °C. 2-(7-Aza-1H-benzotriazole-1-yl)-1,1,3,3-tetramethyluronium hexafluorophosphate (HATU) (1.5 equiv) was added, and the mixture was preactivated by mixing for 10 min, added to the resin, and shaken overnight at room temperature. The resin was washed with NMP (3 × 2 min).

BTC Coupling. The resin was shaken with dibromoethane at 50 °C using a water bath. Fmoc protected amino acids (5 equiv) were dissolved in dibromoethane. Bis(trichloromethyl)carbonate (BTC) (1.67 equiv) was added, and the mixture was cooled to 0 °C. 2,4,6-Collidine (14 equiv) was added dropwise, and the mixture was preactivated by mixing for 1 min, added to the resin, and shaken overnight at 50 °C. The resin was washed with dichloromethane (5 × 2 min).

Alloc Removal. The resin was washed with dichloromethane (2 × 2 min) and dried under vacuum. A solution of 5% AcOH and 2.5% N-methylmorpholine in dichloromethane was added under a stream of argon, and

tetrakis(triphenylphosphine)palladium(0) (0.7 equiv) was added. The mixture was stirred in the dark for 2 h and then washed with 0.5% DIPEA in NMP (3 × 5 min), 0.5% sodium diethyldithiocarbamate trihydrate in NMP (5 × 2 min), NMP (2 × 2 min), and dichloromethane (2 × 2 min).

Urea Cyclization. A solution of BTC (0.33 equiv) in dichloromethane was added to the resin and stirred. After 2 h, DIPEA (2 equiv) was added and the mixture was stirred overnight at room temperature. The resin was washed with dichloromethane (2 × 2 min).

Cyclic Anhydride Coupling. Anhydride (10 equiv) was dissolved in NMP. 4-Dimethylaminopyridine (DMAP) (1 equiv) was added, and the mixture was added to the resin for 2 h. The resin was washed with NMP (2 × 2 min).

Dicarboxylic Acid Coupling. Dicarboxylic acid (10 equiv) and DIC (10 equiv) were dissolved in DMF. The mixture was preactivated by mixing for 30 min. DMAP (1 equiv) was added, and the mixture was added to the resin for 2 h. The resin was washed with NMP (2 × 2 min).

Amide Cyclization. Benzotriazole-1-yl-oxytripyrrolidinophosphonium hexafluorophosphate (PyBOP) (6 equiv) and DIPEA (12 equiv) were dissolved in NMP, and the mixture was added to the resin for 2 h. The mixture was replaced by a mixture of PyBOP (3 equiv) and DIPEA (6 equiv) in NMP and left to stir overnight at room temperature. The resin was washed with NMP (5 × 2 min) and dichloromethane (2 × 2 min).

Cleavage. The resin was washed with dichloromethane (2 × 2 min) and dried under vacuum. A solution of 2.5% TDW and 2.5% triisopropylsilane in trifluoroacetic acid (TFA) was added, and the reaction proceeded for 3 h at room temperature. The solution was separated by filtration, and the resin was rinsed with neat TFA. The TFA mixture was treated with a cooled solution of ether/hexane 1:1, and the peptides were precipitated by centrifugation. The crude peptides were dissolved in acetonitrile/TDW 1:1 solution and lyophilized.

Biological Screening. All peptides and peptidomimetics were screened for inhibition of PKB/Akt in a cell-free radioactive assay and compared with **1** (Tables 2−7). IC$_{50}$ values were determined for the most potent inhibitors, identified in the initial screening (Figure 4).

PKB/Akt Assay. PKB/Akt kinase (HisΔPHPKBEEEFlag) was prepared as described by Klein et al. except that for routine screening the enzyme was only partially purified in one step on Ni-NTA agarose (Qiagen).[60] The radioactive kinase assay was as described by Reuveni et al.[3] except that the reaction mix comprised 50 mM Hepes, pH 7.4, 0.1 mM EGTA, 0.1% (v/v) 2-mercaptoethanol, 10 mM magnesium acetate, 3 μM RPRTSSF peptide, 10 μM [γ^{32}P]ATP (1 μCi/assay well), the inhibitory compound, and 0.005 units of HisΔPHPKBEEEFlag. A stock solution of each peptide was prepared, and the concentration was determined by UV spectrophotometry as described.[61] For initial screening, compounds were tested at three to four concentrations. Compounds that showed significant inhibition at 5 μM or less were retested and IC$_{50}$ values determined using Graphpad Prism 5. **1** was included in every assay, as a standard.

NMR. Samples in lyophilized form were dissolved in 20 mM phosphate buffer and 10% deuterium oxide (Aldrich Chemicals Co., U.S.) to give a concentration of 1.8 mM and pH 6.7. The NMR experiments were performed on a Bruker Avance 600 MHz DMX spectrometer operating at the proton frequency of 600.13 MHz with an *xyz*-gradient coil at 7 °C. The transmitter frequency was set on the HDO signal, which was calibrated at 4.945 ppm. TOSCY[62,63] and NOESY[64,65] experiments were acquired under identical conditions over a range of temperatures between 4 and 32 °C to find optimal conditions for the NMR measurements. Structural data were acquired at 7 °C to reduce peptide motion. TOCSY spectra were recorded using the MLEV-17 pulse scheme for the spin lock at mixing periods of 100 ms with 64 scans per t_1 increment.[66] The NOESY experiments were optimized and finally collected with a mixing time of 250 ms using 176 transients for each t_1. Spectra were processed and analyzed with TopSpin (Bruker Analytische Messtechnik GmbH) and SPARKY (provided by T. D. Goddard and D.

G. Kneller, SPARKY 3, University of California, San Francisco). Zero filling in the indirect dimension and data apodization with shifted squared sine bell window functions in both dimensions were applied prior to Fourier transformation. The baseline was further corrected in the direct dimension with a quadratic polynomial function.

Resonance assignment was done according to the sequential assignment methodology developed by Wüthrich[67] based on the TOCSY and NOESY spectra measured under identical experimental conditions. The volumes of the NOE peaks were calculated by SPARKY, and the three-dimensional structures of the peptides were generated using XPLOR (version 3.856)[68] with patches from within XPLOR for the bridges and ring closure. Chimera[69] was used for visual analysis and presentation. Low energy structures chosen for further analysis had no NOE violations, deviations from ideal bond lengths of less than 0.05 Å, and bond angle deviations from ideality of less than 5°.

Computational Studies. The ANCHORS$_{MAP}$ algorithm[53] was used to predict the most favorable binding sites for Arg residues on the surface of PKB/Akt catalytic domain. The method consists of two steps: (i) The first is a geometry based step, in which subpockets that can accommodate single amino acid side chains are detected on the surface of the protein and amino acid probes are then scattered near them with their Cβ atoms pointing away from the protein surface. This procedure produces a nonrandom yet exhaustive distribution of thousands of probes over the entire protein surface. (ii) The second is an energy-based step in which the positions of probes, initially scattered, are optimized by several cycles of energy minimization and clustering, and their binding energies (ΔG) are estimated by a scoring function adjusted for the context of protein−protein interactions. The scoring function includes an empirical solvation model, van der Waals energy, and an electrostatic energy term corrected for dielectric shielding by a hypothetical protein attached to the probe. The predicted anchoring spots are ranked by their ΔG. The predicted Arg anchoring spots presented in this study are of mean structure using rms$_{min}$ of 3 Å and the default parameters as described.[53] The coordinates of peptide-free structure of PKB/Akt (3D0E) were taken from the Protein Data Bank,[70] and heteroatoms were removed prior to calculations.

Substrate Nomenclature. P0 represents the position of the phospho acceptor residue. P-3 represents the residue three amino acids upstream of P0.

Kinase Nomenclature. PKB/Akt/belongs to the basophilic group of Ser/Thr kinases as previously defined.[54]

■ ASSOCIATED CONTENT

ⓢ Supporting Information. Fingerprint NMR spectra of **1**, HPLC and HRMS characterization of all the compounds, and HPLC traces of selected inhibitors. This material is available free of charge via the Internet at http://pubs.acs.org.

■ AUTHOR INFORMATION

Corresponding Author
*Phone: 972 2 6586181. Fax: 972 2 6416358. E-mail: gilon@vms.huji.ac.il.

■ ACKNOWLEDGMENT

for Biocomputing, Visualization and Informatics at the University of California, San Francisco (supported by NIH Grant P41 RR-01081) and using Discovery Studio 2.5 (Accelrys, Inc). We thank Professor Assaf Friedler, Dr. Noam S. Freeman, and Dr. Zvi Hayouka for helpful discussions.

■ ABBREVIATIONS USED

ACN, acetonitrile; AGBU, Alloc glycine building unit; ANP, phosphoaminophosphonic acid adenylate ester; AT, amino terminus; BN, backbone; BTC, bis(trichloromethyl)carbonate; DIC, N,N'-diisopropylcarbodiimide; DIPEA, diisopropylethylamine; DMAP, 4-dimethylaminopyridine; DMF, N,N-dimethylformamide; Fmoc, 9-fluorenylmethyloxycarbonyl; GBU, N-alkyl(amino functionalized)glycine; GSK3, glycogen synthase kinase 3; HATU, 2-(7-aza-1H-benzotriazole-1-yl)-1,1,3,3-tetramethyluronium hexafluorophosphate; HBTU, 2-(1H-benzotriazole-1-yl)-1,1,3,3-tetramethyluronium hexafluorophosphate; HOAt, 1-hydroxy-7-azabenzotriazole; HOBt,1-hydroxybenzotriazoleMALDI, matrix assisted laser desorption ionization; MBHA, methylbenzhydrylamine; NMP, 1-methyl-2-pyrrolidinone; NMR, nuclear magnetic resonance; NOESY, nuclear Overhauser effect spectroscopy; PKB, protein kinase B; PyBOP, benzotriazole-1-yl-oxytripyrrolidinophosphonium hexafluorophosphate; rmsd, root-mean-square deviation; RP-HPLC, reverse phase high pressure liquid chromatography; SAR, structure—activity relationship; SPPS, solid phase peptide synthesis; TDW, triply distilled water; TFA, trifluoroacetic acid; TOF, time of flight

■ ADDITIONAL NOTE

The abbreviations for amino acids are according to the IUPAC-IUB Commission of Biochemical Nomenclature, http://www.chem.qmul.ac.uk/iupac/AminoAcid/.

■ REFERENCES

(1) Klein, S.; Levitzki, A. Targeting the EGFR and the PKB pathway in cancer. *Curr. Opin. Cell Biol.* **2009**, *21* (2), 185–193.

(2) Davies, S. P.; Reddy, H.; Caivano, M.; Cohen, P. Specificity and mechanism of action of some commonly used protein kinase inhibitors. *Biochem. J.* **2000**, *351*, 95–105.

(3) Reuveni, H.; Livnah, N.; Geiger, T.; Klein, S.; Ohne, O.; Cohen, I.; Benhar, M.; Gellerman, G.; Levitzki, A. Toward a PKB inhibitor: modification of a selective PKA inhibitor by rational design. *Biochemistry* **2002**, *41* (32), 10304–10314.

(4) Godl, K.; Wissing, J.; Kurtenbach, A.; Habenberger, P.; Blencke, S.; Gutbrod, H.; Salassidis, K.; Stein-Gerlach, M.; Missio, A.; Cotten, M.; Daub, H. An efficient proteomics method to identify the cellular targets of protein kinase inhibitors. *Proc. Natl. Acad. Sci. U.S.A.* **2003**, *100* (26), 15434–15439.

(5) Bain, J.; Plater, L.; Elliott, M.; Shpiro, N.; Hastie, C. J.; Mclauchlan, H.; Klevernic, I.; Arthur, J. S. C.; Alessi, D. R.; Cohen, P. The selectivity of protein kinase inhibitors: a further update. *Biochem. J.* **2007**, *408*, 297–315.

(6) Fedorov, O.; Marsden, B.; Pogacic, V.; Rellos, P.; Muller, S.; Bullock, A. N.; Schwaller, J.; Sundstrom, M.; Knapp, S. A systematic interaction map of validated kinase inhibitors with Ser/Thr kinases. *Proc. Natl. Acad. Sci. U.S.A.* **2007**, *104* (51), 20523–20528.

(7) Murray, A. J. Pharmacological PKA inhibition: All may not be what it seems. *Sci. Signaling* **2008**, *1* (22), re4.

(8) Karaman, M. W.; Herrgard, S.; Treiber, D. K.; Gallant, P.; Atteridge, C. E.; Campbell, B. T.; Chan, K. W.; Ciceri, P.; Davis, M. I.; Edeen, P. T.; Faraoni, R.; Floyd, M.; Hunt, J. P.; Lockhart, D. J.; Milanov, Z. V.; Morrison, M. J.; Pallares, G.; Patel, H. K.; Pritchard, S.; Wodicka, L. M.; Zarrinkar, P. P. A quantitative analysis of kinase inhibitor selectivity. *Nat. Biotechnol.* **2008**, *26* (1), 127–132.

(9) Lindsley, C. W.; Barnett, S. F.; Yaroschak, M.; Bilodeau, M. T.; Layton, M. E. Recent progress in the development of ATP-competitive and allosteric akt kinase inhibitors. *Curr. Top. Med. Chem.* **2007**, *7* (14), 1349–1363.

(10) Lindsley, C. W.; Barnett, S. F.; Layton, M. E.; Bilodeau, M. T. The PI3K/Akt pathway: recent progress in the development of ATP-competitive and allosteric Akt kinase inhibitors. *Curr. Cancer Drug Targets* **2008**, *8* (1), 7–18.

(11) Lindsley, C. W. The Akt/PKB family of protein kinases: a review of small molecule inhibitors and progress towards target validation: a 2009 update. *Curr. Top. Med. Chem.* **2010**, *10* (4), 458–477.

(12) Harris, T. E.; Persaud, S. J.; Saermark, T.; Jones, P. M. Effects of myristoylated pseudosubstrate protein—kinase-C peptide inhibitors on insulin-secretion. *Biochem. Soc. Trans.* **1995**, *23* (2), S187–S187.

(13) Alfaro-Lopez, J.; Yuan, W.; Phan, B. C.; Kamath, J.; Lou, Q.; Lam, K. S.; Hruby, V. J. Discovery of a novel series of potent and selective substrate-based inhibitors of p60c-src protein tyrosine kinase: conformational and topographical constraints in peptide design. *J. Med. Chem.* **1998**, *41* (13), 2252–2260.

(14) Levitzki, A. Protein kinase inhibitors as a therapeutic modality. *Acc. Chem. Res.* **2003**, *36* (6), 462–469.

(15) Niv, M. Y.; Rubin, H.; Cohen, J.; Tsirulnikov, L.; Licht, T.; Peretzman-Shemer, A.; Cna'an, E.; Tartakovsky, A.; Stein, I.; Albeck, S.; Weinstein, I.; Goldenberg-Furmanov, M.; Tobi, D.; Cohen, E.; Laster, M.; Ben-Sasson, S. A.; Reuveni, H. Sequence-based design of kinase inhibitors applicable for therapeutics and target identification. *J. Biol. Chem.* **2004**, *279* (2), 1242–1255.

(16) Rubinstein, M.; Niv, M. Y. Peptidic modulators of protein—protein interactions: progress and challenges in computational design. *Biopolymers* **2009**, *91* (7), 505–513.

(17) Litman, P.; Ohne, O.; Ben-Yaakov, S.; Shemesh-Darvish, L.; Yechezkel, T.; Salitra, Y.; Rubnov, S.; Cohen, I.; Senderowitz, H.; Kidron, D.; Livnah, O.; Levitzki, A.; Livnah, N. A novel substrate mimetic inhibitor of PKB/Akt inhibits prostate cancer tumor growth in mice by blocking the PKB pathway. *Biochemistry* **2007**, *46* (16), 4716–4724.

(18) Gante, J. Peptidomimetics—tailored enzyme-inhibitors. *Angew. Chem., Int. Ed. Engl.* **1994**, *33* (17), 1699–1720.

(19) Naider, F.; Goodman, M. Historical Aspects. In *Synthesis of Peptides and Peptidomimetics*, 4th ed.; Goodman, M., Toniolo, C., Moroder, L., Felix, A., Eds.; Thieme: Stuttgart, Germany, 2002; Vol. E22a, pp 1—16.

(20) Ahn, J. M.; Boyle, N. A.; MacDonald, M. T.; Janda, K. D. Peptidomimetics and peptide backbone modifications. *Mini-Rev. Med. Chem.* **2002**, *2* (5), 463–473.

(21) Vagner, J.; Qu, H. C.; Hruby, V. J. Peptidomimetics, a synthetic tool of drug discovery. *Curr. Opin. Chem. Biol.* **2008**, *12* (3), 292–296.

(22) Ruan, F. Q.; Chen, Y. Q.; Itoh, K.; Sasaki, T.; Hopkins, P. B. Synthesis of peptides containing unnatural, metal-ligating residues: aminodiacetic acid as a peptide side chain. *J. Org. Chem.* **1991**, *56* (14), 4347–4354.

(23) Giblin, M. F.; Wang, N.; Hoffman, T. J.; Jurisson, S. S.; Quinn, T. P. Design and characterization of alpha-melanotropin peptide analogs cyclized through rhenium and technetium metal coordination. *Proc. Natl. Acad. Sci. U.S.A.* **1998**, *95* (22), 12814–12818.

(24) Miller, S. J.; Grubbs, R. H. Synthesis of conformationally restricted amino acids and peptides employing olefin metathesis. *J. Am. Chem. Soc.* **1995**, *117* (21), 5855–5856.

(25) Miller, S. J.; Blackwell, H. E.; Grubbs, R. H. Application of ring-closing metathesis to the synthesis of rigidified amino acids and peptides. *J. Am. Chem. Soc.* **1996**, *118* (40), 9606–9614.

(26) Stewart, M. L.; Fire, E.; Keating, A. E.; Walensky, L. D. The MCL-1 BH3 helix is an exclusive MCL-1 inhibitor and apoptosis sensitizer. *Nat. Chem. Biol.* **2010**, *6* (8), 595–601.

(27) Veber, D. F.; Freidinger, R. M.; Perlow, D. S.; Paleveda, W. J.; Holly, F. W.; Strachan, R. G.; Nutt, R. F.; Arison, B. H.; Homnick, C.; Randall, W. C.; Glitzer, M. S.; Saperstein, R.; Hirschmann, R. A potent cyclic hexapeptide analog of somatostatin. *Nature* **1981**, *292* (5818), 55–58.

(28) Samanen, J.; Ali, F.; Romoff, T.; Calvo, R.; Sorenson, E.; Vasko, J.; Storer, B.; Berry, D.; Bennett, D.; Strohsacker, M.; Powers, D.; Stadel, J.; Nichols, A. Development of a small RGD peptide fibrinogen receptor antagonist with potent antiaggregatory activity in vitro. *J. Med. Chem.* **1991**, *34* (10), 3114–3125.

(29) Kopple, K. D.; Baures, P. W.; Bean, J. W.; Dambrosio, C. A.; Hughes, J. L.; Peishoff, C. E.; Eggleston, D. S. Conformations of Arg-Gly-Asp containing heterodetic cyclic peptides: solution and crystal studies. *J. Am. Chem. Soc.* **1992**, *114* (24), 9615–9623.

(30) Cheng, S.; Craig, W. S.; Mullen, D.; Tschopp, J. F.; Dixon, D.; Pierschbacher, M. D. Design and synthesis of novel cyclic RGD-containing peptides as highly potent and selective integrin alpha(IIb)beta(3) antagonists. *J. Med. Chem.* **1994**, *37* (1), 1–8.

(31) Ali, F. E.; Bennett, D. B.; Calvo, R. R.; Elliott, J. D.; Hwang, S. M.; Ku, T. W.; Lago, M. A.; Nichols, A. J.; Romoff, T. T.; Shah, D. H.; Vasko, J. A.; Wong, A. S.; Yellin, T. O.; Yuan, C. K.; Samanen, J. M. Conformationally constrained peptides and semipeptides derived from RGD as potent inhibitors of the platelet fibrinogen receptor and platelet aggregation. *J. Med. Chem.* **1994**, *37* (6), 769–780.

(32) Scarborough, R. M.; Gretler, D. D. Platelet glycoprotein IIb-IIIa antagonists as prototypical integrin blockers: novel parenteral and potential oral antithrombotic agents. *J. Med. Chem.* **2000**, *43* (19), 3453–3473.

(33) Weckbecker, G.; Lewis, I.; Albert, R.; Schmid, H. A.; Hoyer, D.; Bruns, C. Opportunities in somatostatin research: biological, chemical and therapeutic aspects. *Nat. Rev. Drug Discovery* **2003**, *2* (12), 999–1017.

(34) Hruby, V. J.; al-Obeidi, F.; Kazmierski, W. Emerging approaches in the molecular design of receptor-selective peptide ligands: conformational, topographical and dynamic considerations. *Biochem. J.* **1990**, *268* (2), 249–262.

(35) Demmer, O.; Frank, A. O.; Kessler, H. Design of Cyclic Peptides. In *Peptide and Protein Design for Biopharmaceutical Applications*; Jensen, K. J., Ed.; John Wiley and Sons Ltd.: Hoboken, NJ, 2009; pp 133–176.

(36) Gilon, C.; Halle, D.; Chorev, M.; Selinger, Z.; Byk, G. Backbone cyclization: a new method for conferring conformational constraint on peptides. *Biopolymers* **1991**, *31* (6), 745–750.

(37) Fesik, S. W.; Gampe, R. T.; Eaton, H. L.; Gemmecker, G.; Olejniczak, E. T.; Neri, P.; Holzman, T. F.; Egan, D. A.; Edalji, R.; Simmer, R.; Helfrich, R.; Hochlowski, J.; Jackson, M. NMR studies of [U-^{13}C]cyclosporin A bound to cyclophilin: bound conformation and portions of cyclosporine involved in binding. *Biochemistry* **1991**, *30* (26), 6574–6583.

(38) Heavner, G. A.; Audhya, T.; Doyle, D.; Tjoeng, F. S.; Goldstein, G. Biologically active conformations of thymopentin: studies with conformationally restricted analogs. *Int. J. Pept. Protein Res.* **1991**, *37* (3), 198–209.

(39) Weber, C.; Wider, G.; Vonfreyberg, B.; Traber, R.; Braun, W.; Widmer, H.; Wuthrich, K. The NMR structure of cyclosporine A bound to cyclophilin in aqueous solution. *Biochemistry* **1991**, *30* (26), 6563–6574.

(40) Grdadolnik, S. G.; Mierke, D. F.; Byk, G.; Zeltser, I.; Gilon, C.; Horst, K.; Kessler, H. Comparison of the conformation of active and nonactive backbone cyclic analogs of substance P as a tool to elucidate features of the bioactive conformation: NMR and molecular dynamics in DMSO and water. *J. Med. Chem.* **1994**, *37* (14), 2145–2152.

(41) Gazal, S.; Gelerman, G.; Ziv, O.; Karpov, O.; Litman, P.; Bracha, M.; Afargan, M.; Gilon, C. Human somatostatin receptor specificity of backbone-cyclic analogues containing novel sulfur building units. *J. Med. Chem.* **2002**, *45* (8), 1665–1671.

(42) Qvit, N.; Hatzubai, A.; Shalev, D. E.; Friedler, A.; Ben-Neriah, Y.; Gilon, C. Design and synthesis of backbone cyclic phosphorylated peptides: the IkappaB model. *Biopolymers* **2009**, *91* (2), 157–168.

(43) Hess, S.; Ovadia, O.; Shalev, D. E.; Senderovich, H.; Qadri, B.; Yehezkel, T.; Salitra, Y.; Sheynis, T.; Jelinek, R.; Gilon, C.; Hoffman, A. Effect of structural and conformation modifications, including backbone cyclization, of hydrophilic hexapeptides on their intestinal permeability and enzymatic stability. *J. Med. Chem.* **2007**, *50* (24), 6201–6211.

(44) Hess, S.; Linde, Y.; Ovadia, O.; Safrai, E.; Shalev, D. E.; Swed, A.; Halbfinger, E.; Lapidot, T.; Winkler, I.; Gabinet, Y.; Faier, A.; Yarden, D.; Xiang, Z.; Portillo, F. P.; Haskell-Luevano, C.; Gilon, C.; Hoffman, A. Backbone cyclic peptidomimetic melanocortin-4 receptor agonist as a novel orally administrated drug lead for treating obesity. *J. Med. Chem.* **2008**, *51* (4), 1026–1034.

(45) Tal-Gan, Y.; Freeman, N. S.; Klein, S.; Levitzki, A.; Gilon, C. Synthesis and structure—activity relationship studies of peptidomimetic PKB/Akt inhibitors: the significance of backbone interactions. *Bioorg. Med. Chem.* **2010**, *18* (8), 2976–2985.

(46) Freeman, N. S.; Tal-Gan, Y.; Klein, S.; Levitzki, A.; Gilon, C. Microwave-assisted solid phase aza-peptide synthesis: aza-scan of a PKB/Akt inhibitor using aza-arginine and aza-proline precursors. *J. Org. Chem.* **2011**, *76* (9), 3078–3085.

(47) Hurevich, M.; Tal-Gan, Y.; Klein, S.; Barda, Y.; Levitzki, A.; Gilon, C. Novel method for the synthesis of urea backbone cyclic peptides using new Alloc-protected glycine building units. *J. Pept. Sci.* **2010**, *16* (4), 178–185.

(48) Ben-Shimon, A.; Niv, M. Y. Unpublished results.

(49) Gilon, C.; Tal-Gan, Y.; Klein, S.; Levitzki, A. Peptidomimetic inhibitors of PKB/Akt anti cancer drug leads; US provisional application 61/286141.

(50) Yang, J.; Cron, P.; Good, V. M.; Thompson, V.; Hemmings, B. A.; Barford, D. Crystal structure of an activated Akt/protein kinase B ternary complex with GSK3-peptide and AMP-PNP. *Nat. Struct. Biol.* **2002**, *9* (12), 940–944.

(51) Alessi, D. R.; Caudwell, F. B.; Andjelkovic, M.; Hemmings, B. A.; Cohen, P. Molecular basis for the substrate specificity of protein kinase B: comparison with MAPKAP kinase-1 and p70 S6 kinase. *FEBS Lett.* **1996**, *399* (3), 333–338.

(52) Obata, T.; Yaffe, M. B.; Leparc, G. G.; Piro, E. T.; Maegawa, H.; Kashiwagi, A.; Kikkawa, R.; Cantley, L. C. Peptide and protein library screening defines optimal substrate motifs for AKT/PKB. *J. Biol. Chem.* **2000**, *275* (46), 36108–36115.

(53) Ben-Shimon, A.; Eisenstein, M. Computational mapping of anchoring spots on protein surfaces. *J. Mol. Biol.* **2010**, *402* (1), 259–277.

(54) Pinna, L. A.; Ruzzene, M. How do protein kinases recognize their substrates? *Biochim Biophys. Acta, Mol. Cell Res.* **1996**, *1314* (3), 191–225.

(55) Madhusudan; Trafny, E. A.; Xuong, N. H.; Adams, J. A.; Ten Eyck, L. F.; Taylor, S. S.; Sowadski, J. M. cAMP-dependent protein kinase: crystallographic Insights into Substrate Recognition and Phosphotransfer. *Protein Sci.* **1994**, *3* (2), 176–187.

(56) Niv, M. Y.; Weinstein, H. A flexible docking procedure for the exploration of peptide binding selectivity to known structures and homology models of PDZ domains. *J. Am. Chem. Soc.* **2005**, *127* (40), 14072–14079.

(57) Cheng, S.; Niv, M. Y. Molecular dynamics simulations and elastic network analysis of protein kinase B (Akt/PKB) inactivation. *J. Chem. Inf. Model.* **2010**, *50* (9), 1602–1610.

(58) Chan, W. C.; White, P. D. *Fmoc Solid Phase Peptide Synthesis*; Oxford University Press: Oxford, U.K., 2000; Vol. 222.

(59) Byk, G.; Halle, D.; Zeltser, I.; Bitan, G.; Selinger, Z.; Gilon, C. Synthesis and biological activity of NK-1 selective, N-backbone cyclic analogs of the C-terminal hexapeptide of substance P. *J. Med. Chem.* **1996**, *39* (16), 3174–3178.

(60) Klein, S.; Geiger, T.; Linchevski, I.; Lebendiker, M.; Itkin, A.; Assayag, K.; Levitzki, A. Expression and purification of active PKB kinase from *Escherichia coli*. *Protein Expression Purif.* **2005**, *41* (1), 162–169.

(61) Gill, S. C.; von Hippel, P. H. Calculation of protein extinction coefficients from amino acid sequence data. *Anal. Biochem.* **1989**, *182* (2), 319–326.

(62) Piotto, M.; Saudek, V.; Sklenar, V. Gradient-tailored excitation for single-quantum NMR spectroscopy of aqueous solutions. *J. Biomol. NMR* **1992**, *2* (6), 661–665.

(63) Sklenar, V.; Piotto, M.; Leppik, R.; Saudek, V. Gradient-tailored water suppression for H-1-N-15 HSQC experiments optimized to retain full sensitivity. *J. Magn. Reson., Ser. A* **1993**, *102* (2), 241–245.

(64) Kumar, A.; Ernst, R. R.; Wuthrich, K. A two-dimensional nuclear Overhauser enhancement (2D NOE) experiment for the elucidation of complete proton—proton cross-relaxation networks in biological macromolecules. *Biochem. Biophys. Res. Commun.* **1980**, *95* (1), 1–6.

(65) Liu, M. L.; Mao, X. A.; Ye, C. H.; Huang, H.; Nicholson, J. K.; Lindon, J. C. Improved WATERGATE pulse sequences for solvent suppression in NMR spectroscopy. *J. Magn. Reson.* **1998**, *132* (1), 125–129.

(66) Bax, A.; Davis, D. G. Mlev-17-based two-dimensional homonuclear magnetization transfer spectroscopy. *J. Magn. Reson., Ser, A* **1985**, *65* (2), 355–360.

(67) Wuthrich, K. *NMR of Proteins and Nucleic Acids*; John Wiley & Sons: New York, 1986; p 320.

(68) Nilges, M.; Kuszewski, J.; Brunger, A. *Sampling Properties of Simulated Annealing and Distance Geometry*; Plenum Press: New York, 1991; p 451−455.

(69) Pettersen, E. F.; Goddard, T. D.; Huang, C. C.; Couch, G. S.; Greenblatt, D. M.; Meng, E. C.; Ferrin, T. E. UCSF chimera: a visualization system for exploratory research and analysis. *J. Comput. Chem.* **2004**, *25* (13), 1605–1612.

(70) Berman, H. M.; Westbrook, J.; Feng, Z.; Gilliland, G.; Bhat, T. N.; Weissig, H.; Shindyalov, I. N.; Bourne, P. E. The Protein Data Bank. *Nucleic Acids Res.* **2000**, *28* (1), 235–242.